Rh(III)-Catalyzed *N*-Amino-Directed C-H Coupling with 3-Methyleneoxetan-2-Ones for 1,2-Dihydroquinoline-3-Carboxylic Acid Synthesis

Renpeng Zhou, Shuaixin Fan, Lili Fang, Benfa Chu, and Jin Zhu*

Department of Polymer Science and Engineering, School of Chemistry and Chemical Engineering, State Key Laboratory of Coordination Chemistry, Nanjing University, Nanjing 210023, China.

*Corresponding Author. E-mail: jinz@nju.edu.cn.

Abstract: Polarity analysis is important for the deduction of organic reactivity but is largely restricted in the static polarity analysis regime. Dynamic polarity analysis is proposed herein as an expansive tool for quest into both static polarity and transient polarity, allowing the revelation of an augmented pool of reactivity patterns. Through this analysis formalism, polarity matching has been established for Rh(III)-catalyzed *N*-amino-directed C-H coupling with 3-methyleneoxetan-2-ones providing efficient access to 1,2-dihydroquinoline-3-carboxylic acids. The identified reaction, by virtue of the internal oxidative mechanism, showcases a mild reaction condition (room temperature), a short reaction time (2 h), and a generally high product yield. Taken together, the integration of static and dynamic polarity analysis creates a unified foundational framework for reactivity deduction and reactivity classification, in both organic and organometallic chemistry.

Keywords: Polarity analysis; Static polarity analysis; Dynamic polarity analysis; Rhodium catalysis; C-H coupling.

Introduction

Polarity matching is a central guiding principle in the predictive deduction of potential reactivity between two organic molecules.[1-3] The opposite polarity between the two sites in the reaction partners, one electronically rich (nucleophilic) and one electronically poor (electrophilic), creates a working mechanism for their engagement into a bonding state. As such, polarity analysis, the formal examination and assignment of electronic character of organic molecule sites and corresponding electronic character complementarity, has developed into a core synthetic planning practice.[4-8] Thus far, polarity analysis is executed primarily in the realm of conventional organic chemistry and in the form of static polarity analysis, assignment of electronic character exclusively based on the electronegativity (with resonance effect included) of each site (static polarity: regular polarity and umpolung polarity inversion) and associated complementarity.[9-13] This mechanistic framework of reactivity deduction, despite its tremendous synthetic utility, contributes to the derivation of only a rather limited portion of reactivity patterns observed in organic reactions. An alternative mode of reactivity deduction, dynamic polarity analysis, might allow the revelation of a massive pool of otherwise hidden reactivity patterns. Dynamic polarity analysis refers to the electronic character assignment of both static polarity and transient polarity (transient species-generated polarity, other than static polarity), at each site, and associated complementarity. It is important to emphasize that transient polarity can be frequently distinct from the static polarity. An oxidative or reductive setup is equivalent to the inversion of site polarity for one reaction partner, enabling the creation of formal reactivity between two sites of seemingly identical polarity.

Transition metal catalysis in the realm of organometallic chemistry has been an

incessant source of inspiration for the development of new organic reactions.[14-17] A hallmark of this type of catalytic events is the vast population of diversified transient species and accordingly, varied transient polarity. In this regard, dynamic polarity analysis can contribute, as an ideal mechanistic handle, to the derivation of organometallic reactivity. Organometallic chemistry has been traditionally depicted by several elementary events (e.g., oxidative addition, reductive elimination, insertion, elimination).[18] This mechanistic framework, albeit largely effective, is not in sync with that used in organic chemistry. Polarity analysis provides an integrated mechanistic framework for unifying organic chemistry and organometallic chemistry. This framework is closely related to the typically adopted step-by-step bond transformation mechanistic framework but perceived to be more deterministic and less subjective, and thus represents a more foundational, invariant scientific concept. Invariant has been a broadly used mathematics concept, conceived as a property of a mathematical object that remains unchanged upon a specific operation. Herein, the unification of static and dynamic polarity analysis can establish an invariant formalism for reactivity deduction and reactivity classification. An invariant here from the polarity analysis perspective is conceived to be a set of polarity-matched sites that are completely defined, regardless of bond transformation mechanisms, as a prerequisite for converting two reaction partners into a specific product. A note to add is that polarity analysis can lead to the identification of a multitude of polarity-matched reactivity courses and product structural sets. This comprehensive information can serve as a necessary condition, not as a sufficient condition, for guiding judgment on the viability of reaction development targeting a specific product.

Scheme 1. Polarity analysis, including static polarity analysis and dynamic polarity analysis, as illustrated with the coupling of 1-methyl-1-phenylhydrazine (1a) and 3-methyleneoxetan-2-one (R = Ph(CH$_2$)$_2$, 2a) (3a as the product).

(I) Notion for polarity analysis as proposed herein

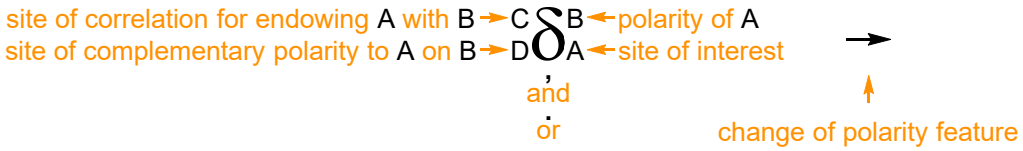

(II) Static polarity analysis

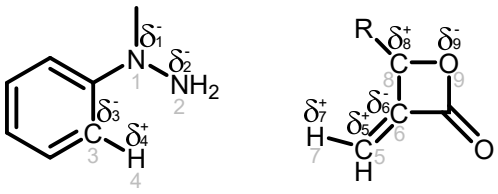

(III) Dynamic polarity analysis

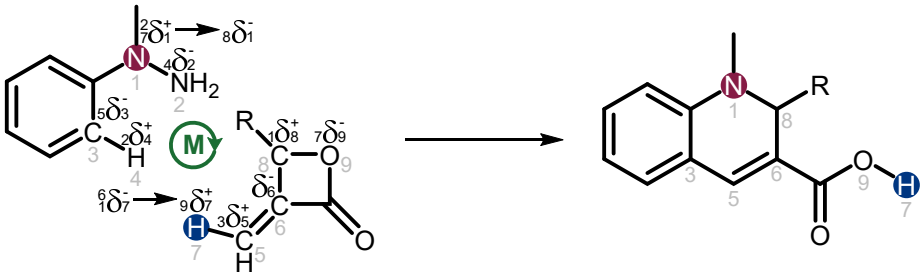

Results and Discussion

We have been working on transition metal-catalyzed, directed C-H bond activation and uncovered a particularly potent directing group, *N*-amino (hydrazine) group.[19-22] As part of our continued effort for expanding its reactivity pattern, we have turned our attention to the coupling with 3-methyleneoxetan-2-ones. Based on the currently accumulated expertise on electronegativity and transient species, in contrast to static polarity analysis, dynamic polarity analysis (Scheme 1) informs distinct polarity attributes for 1-methyl-1-phenylhydrazine (**1a**) and 3-methylene-4-phenethyloxetan-2-one (**2a**) under transition metal catalysis: δ^+ for N1, δ^- for N2 (as in N1-N2-bonded state when partnering with organometallic species; or viewed as the inversed polarity δ^+ for N1 from the original static polarity δ^- for N1, due to the internal oxidative setup; N2 as site of correlation to N1), and subsequent transition to

δ^- for N1 (as in N1-N2-debonded state); δ^- for C3 and δ^+ for H4; δ^+ for C5, δ^- for C6, δ^- for H7 (originated from δ^- of C6, as in transition-metal-H7 hydride-bonded state; C6 as site of correlation to H7), and subsequent transition to δ^+ for H7 (as in N1-H7-bonded state); δ^+ for C8 and δ^- for O9. The static polarity includes N1 (δ^-), N2 (δ^-), C3 (δ^-), H4 (δ^+), C5 (δ^+), C6 (δ^-), H7 (δ^+), C8 (δ^+), O9 (δ^-), and the dynamic polarity includes N1 (δ^+), H7 (δ^-). Polarity matching under dynamic polarity analysis regime can be established for N1 (δ^+)/H7 (δ^-), N2 (δ^-)/H4 (δ^+), C3 (δ^-)/C5 (δ^+), N1 (δ^-)/C8 (δ^+), and H7 (δ^+)/O9 (δ^-), resulting in the formation of product

Scheme 2. Rh(III)-catalyzed C-H coupling with 3-methyleneoxetan-2-one for the synthesis of carboxyl group-functionalized azaheterocycle.

(I) Previous work

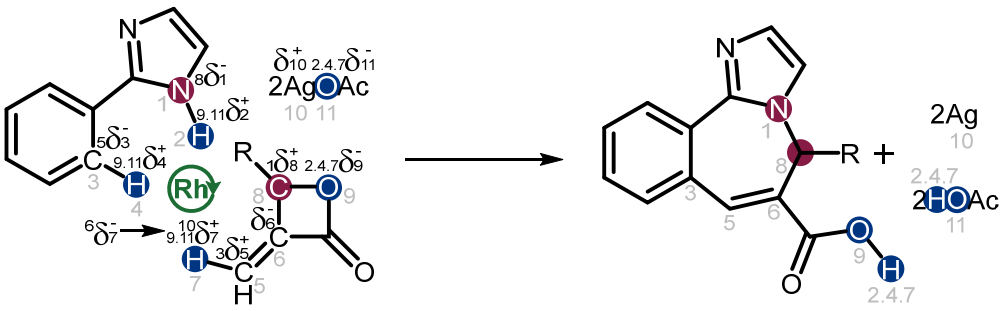

Harsh reaction conditions
Transition metal external oxidant
100 °C (60 °C above solvent boiling point)
Slow (10 h)
Generally lower-yielding

(II) This work

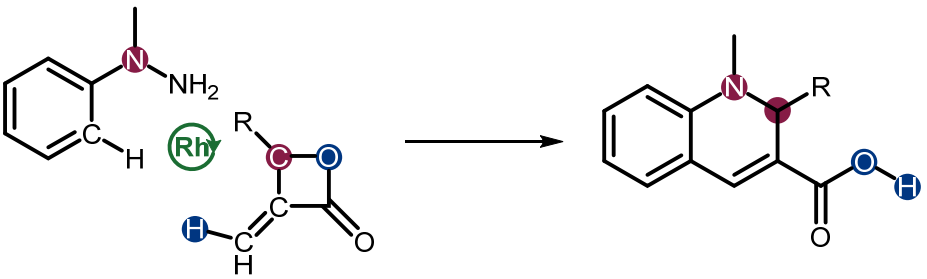

Mild reaction conditions
Internal oxidant
Room temperature
Fast (2 h)
Generally higher-yielding

1-methyl-2-phenethyl-1,2-dihydroquinoline-3-carboxylic acid (**3a**). Herein, we report the implementation of a Rh(III) catalytic protocol for the formal achievement of such a polarity-matched reactivity.

The synthesis of a heterocyclic skeleton derivatized with a strongly coordinating functional group through transition metal-catalyzed, directed C-H bond activation is a highly sought after yet inherently challenging goal.[23-25] The potential competition for coordination from the strongly coordinating functional group can likely disrupt the directing group-directed C-H bond activation process.[26-28] Herein (Scheme 2), dynamic polarity analysis reveals a reactivity course for **1a** and **2a**, with carboxyl group cyclically masked against coordination before *N*-amino-directed, Rh(III)-catalyzed C-H bond activation and ring-opening-displayed in the open-chain format afterwards, that enables access to **3a**. **3a** exemplifies a unique structural type as thus far, no carboxyl group-functionalized azaheterocycle has been synthesized through internal oxidative ring closure based on directed C-H coupling with 3-methyleneoxetan-2-ones.[29-34] For its production, a polarity-matched invariant, N1 (δ^+)/H7 (δ^-), N2 (δ^-)/H4 (δ^+), N1 (δ^-)/C8 (δ^+), H7 (δ^+)/O9 (δ^-), is required here, and this type of invariant is lacking in all previous systems.

Our reaction development commences with the coupling of **1a** and **2a**, at the 0.2 mmol scale, under Ru(II) catalysis. Even with extensive optimization, the synthesis can only reach a maximum yield of merely 37% for **3a** after 12 h, 5 mol% $[RuCl_2(p\text{-cymene})_2]_2$/1.0 equiv $Zn(OTf)_2$-participated room temperature (rt) reaction in MeOH. A temperature rise to 40 ºC lowers the yield to 32%. Without achieving a satisfactory result under Ru(II), we elect to switch the transitional metal to Rh(III). With the replacement of 5 mol% $[RuCl_2(p\text{-cymene})_2]_2$ by 2 mol% $[RhCp^*Cl_2]_2$, the yield improves to 77%. A variation of solvent to either CF_3CH_2OH (TFE) (49%) or CH_3CN

(34%) impedes the reaction. Further solvent screening identifies the solvent of choice to be $ClCH_2CH_2Cl$ (DCE), with the yield escalated to 93%. A reduction of $Zn(OTf)_2$ quantity to 0.2 equiv (67%) exerts a negative impact. Analogous to the Ru(II) system, a temperature rise to 40 °C also decreases the yield (85%). The yield stays approximately the same (94%) even with the reaction time shortened to 2 h, which is taken as the optimum condition. A scale-up reaction at the 10 mmol level sustains the yield at 82% (0.5 mol% $[RhCp^*Cl_2]_2$, 12 h). Rh(III) catalysis is critical as without $[RhCp^*Cl_2]_2$, essentially no **3a** can be detected. An adjustment of $Zn(OTf)_2$ to either $Zn(OAc)_2$ (74%), LiOTf (84%), NaOAc (45%), or HOAc (84%) is not beneficial.

Scheme 3. Substrate scope of hydrazines.[a,b]

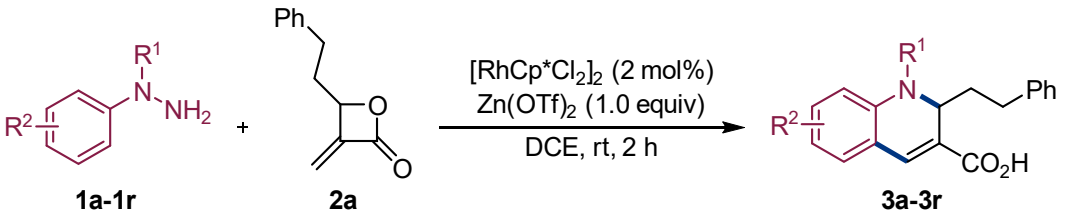

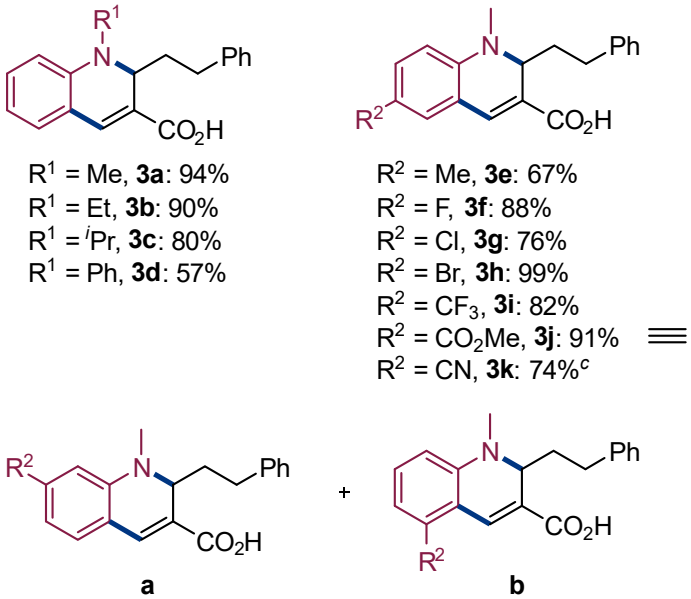

[a]Reaction conditions: **1a-1r** (0.2 mmol, 1.0 equiv), **2a** (0.24 mmol, 1.2 equiv), DCE (2.0 mL), rt, under N_2, 2 h. [b]Isolated yields. [c]MeOH, 12 h.

With the experimental condition optimized, we proceed to the examination of substrate scope. The hydrazine scope, with varied substituent attached to the N atom and phenyl ring of **1a**, is first investigated by reacting with **2a** (Scheme 3). For the N substitution, steric hindrance likely plays a dictating role in the product yield. Thus, the yield is 90% for Et (**1b**), 80% for ^{i}Pr (**1c**), and 57% for Ph (**1d**). For the *para* substitution, the reaction can progress well with both electron-donating and electron-withdrawing groups. The electronically rich Me group (**1e**) can afford a yield of 67%. The electronically poor halogen group shows an intermediate yield for F (**1f**, 88%), a lowest yield for Cl (**1g**, 76%), and a highest yield for Br (**1h**, 99%). Within the strongly electron-withdrawing groups, the yield is intermediate for CF_3 (**1i**, 82%), highest for CO_2Me (**1j**, 91%; structure unambiguously confirmed by single-crystal X-ray diffraction analysis), and lowest for CN (**1k**, MeOH, 12 h reaction, 74%). For the *ortho* substitution, the Me group (**1l**, 80%) is superior to the *para* counterpart, whereas the F group (**1m**, 74%) is inferior to the *para* counterpart. The *meta* substitution generally exhibits a mixture product derived from two non-equivalent C-H sites. The combined yields for Me (**1n**, 78%, 1:0.07) and F (**1o**, 74%, 1:0.17) are comparable to the *ortho* counterparts, with a notable distinction between the two C-H sites (C-H site *para* to the substituent dominating over the *ortho* one). For the Cl group (**1p**, 62%, 1:0.83), the contrast between the two C-H sites is diminished. A single product excels for the CF_3 group (**1q**, 86%). A simultaneous N and phenyl ring substitution arranged as a cyclic fused moiety (**1r**) maintains the yield at 79%, suggesting the ability to effect C-H bond activation even with the rigidified *N*-amino group. The products synthesized herein are frequently fluorescent, with the absorption maxima at ~380 nm (**3a**, **3i**, **3j**, **3k**; **3b**, **3r**, with a longer-wavelength shoulder component), and emission maxima at either ~490 nm (**3a**, **3i**, **3j**, **3k**) or ~520 nm (**3b**,

3r). Apparently, whereas an electron-withdrawing group does not negatively affect the π-conjugated electronic properties, an electron-donating group presents a positive effect on the π-conjugation.

Scheme 4. Substrate scope of 3-methyleneoxetan-2-ones.[a,b]

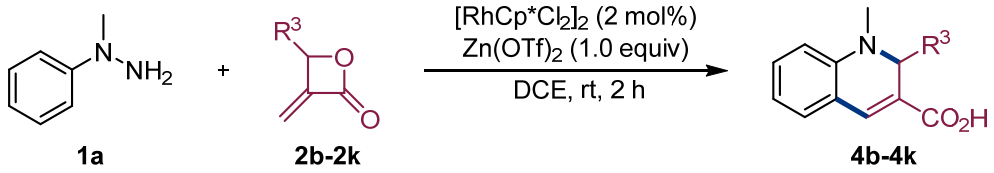

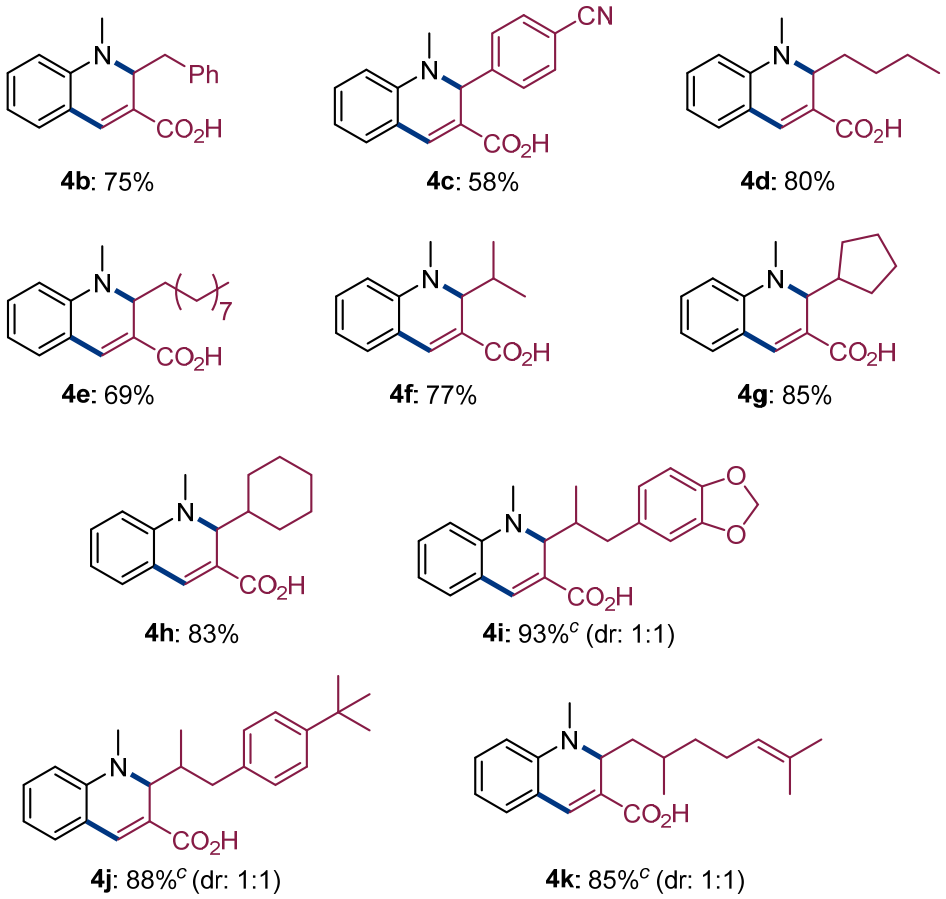

[a]Reaction conditions: **1a** (0.2 mmol, 1.0 equiv), **2b**-**2k** (0.24 mmol, 1.2 equiv), DCE (2.0 mL), rt, under N_2, 2 h. [b]Isolated yields. [c]Inseparable mixture of isomers, with the ratio determined by ^{1}H NMR.

With the hydrazine scope surveyed, the 3-methyleneoxetan-2-one scope is next inspected by employing **1a** as the coupling partner (Scheme 4). A shortening of one CH_2 from the phenethyl group of **2a** to the benzyl group (**2b**) reduces the yield to 75%. A further shortening to the 4-cyanophenyl group (**2c**) drops the yield to 58%. A

complete alteration to the ^{n}Bu group (**2d**) witnesses a yield of 80%. A lengthening to the *n*-nonyl group (**2e**) depresses the yield to 69%. Steric hindrance is not a constraint on the product yield. The yield is 77% with the ^{i}Pr group (**2f**) and comparatively higher with the cyclopentyl (**2g**, 85%) and cyclohexyl (**2h**, 83%) groups. The substitution with an asymmetrically branched group invariably furnishes a 1:1 diastereomeric mixture product. Both 1-(benzo[*d*][1,3]dioxol-5-yl)propan-2-yl (**2i**, 93%) and 1-(4-(tert-butyl)phenyl)propan-2-yl (**2j**, 88%) groups deliver superior yields. With the 2,6-dimethylhept-5-en-1-yl group (**2k**, 85%), the extra alkene moiety does not interfere with the reaction and remains intact.

With the broad substrate scope demonstrated, a series of experiments for unraveling the catalytic cycle is then performed (Scheme 5). An attempted reaction of **1a** with open-chained 3-hydroxy-2-methylene-5-phenylpentanoic acid (**5**) or methyl 3-hydroxy-2-methylene-5-phenylpentanoate (**6**) fails to generate **3a**, highlighting the pivotal contribution of cyclic masking to the product formation. C-H bond activation is considered to be a key step in the catalytic cycle. However, a C-H bond-activated rhodacycle, **1a-Rh-Cl**, is stoichiometrically virtually non-reactive toward **2a**. In contrast, **1a-Rh-Cl** can catalyze the reaction between **1a** and **2a** to an identical **3a** yield of 94% as $[RhCp^*Cl_2]_2$. An addition of **1a** to the stoichiometric mixture of **1a-Rh-Cl** and **2a** can drive the reaction to **3a** (70%).

Taken together, an associative covalent relay catalysis[35,36] is proposed to be operative herein (Scheme 6). The following catalytic sequence, in the conventional bond transformation mechanistic framework, is therefore envisioned: a ligand exchange between $[RhCp^*Cl_2]_2$ and $Zn(OTf)_2$ gives $[RhCp^*(OTf)]^+$, C-H bond activation of **1a** with $[RhCp^*(OTf)]^+$ produces **I**, a **2a** binding with **I** and migratory insertion afford **II**, *β*-hydride elimination of **II** furnishes **III**, N-N bond cleavage of

III in partnering with the binding of incoming **1a** releases **IV** and regenerates **I**, ring closure and ring opening of **IV** deliver **3a**.

Scheme 5. Mechanistic experiments.

(I) Control experiments

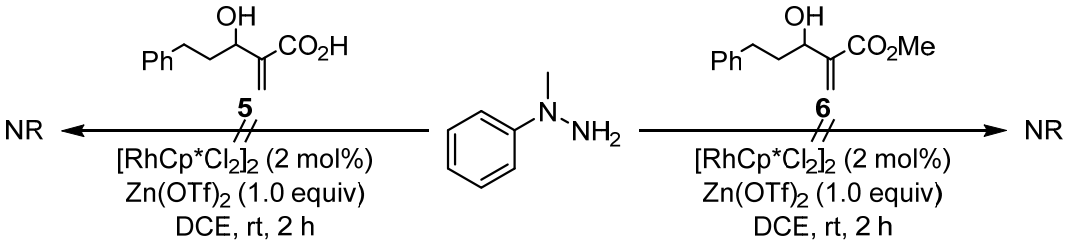

(II) Mechanistic studies involving rhodacycle

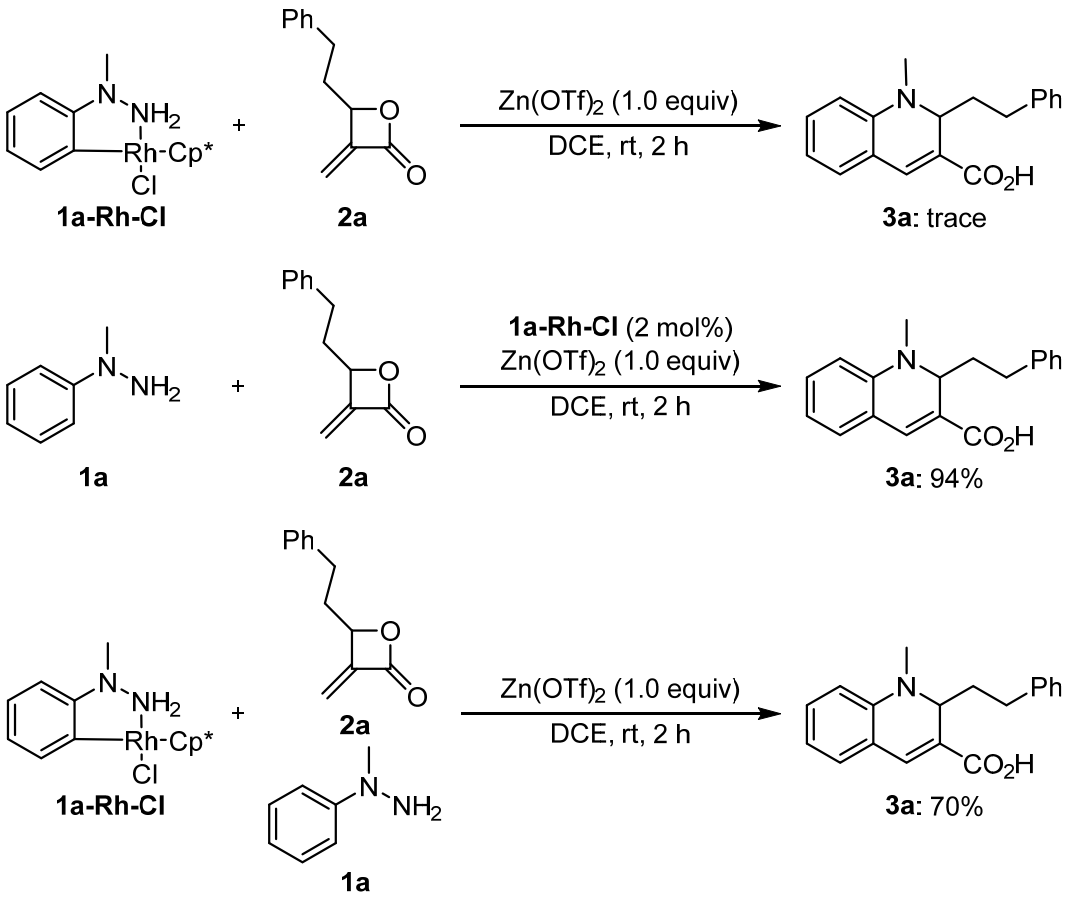

Conclusion

In summary, dynamic polarity analysis has been proposed herein as an effective mechanistic framework for predictive deduction of potential reactivity in the realm of organometallic chemistry. Polarity matching has allowed the derivation of a reactivity

course for *N*-amino-directed C-H coupling with 3-methyleneoxetan-2-ones via an internal oxidative mechanism and synthesis of carboxyl group-functionalized heterocyclic structures, 1,2-dihydroquinoline-3-carboxylic acids. As a demonstration of the effectiveness of such a polarity matching-based reactivity derivation, a Rh(III) catalytic protocol has been developed for implementing the reaction. The integration of static and dynamic polarity analysis has established polarity analysis as a unified foundational framework for rationalizing reactivity, including reactivity deduction and reactivity classification (with invariant formalism), in both organic and organometallic chemistry.

Scheme 6. Proposed reaction mechanism in the conventional bond transformation framework.

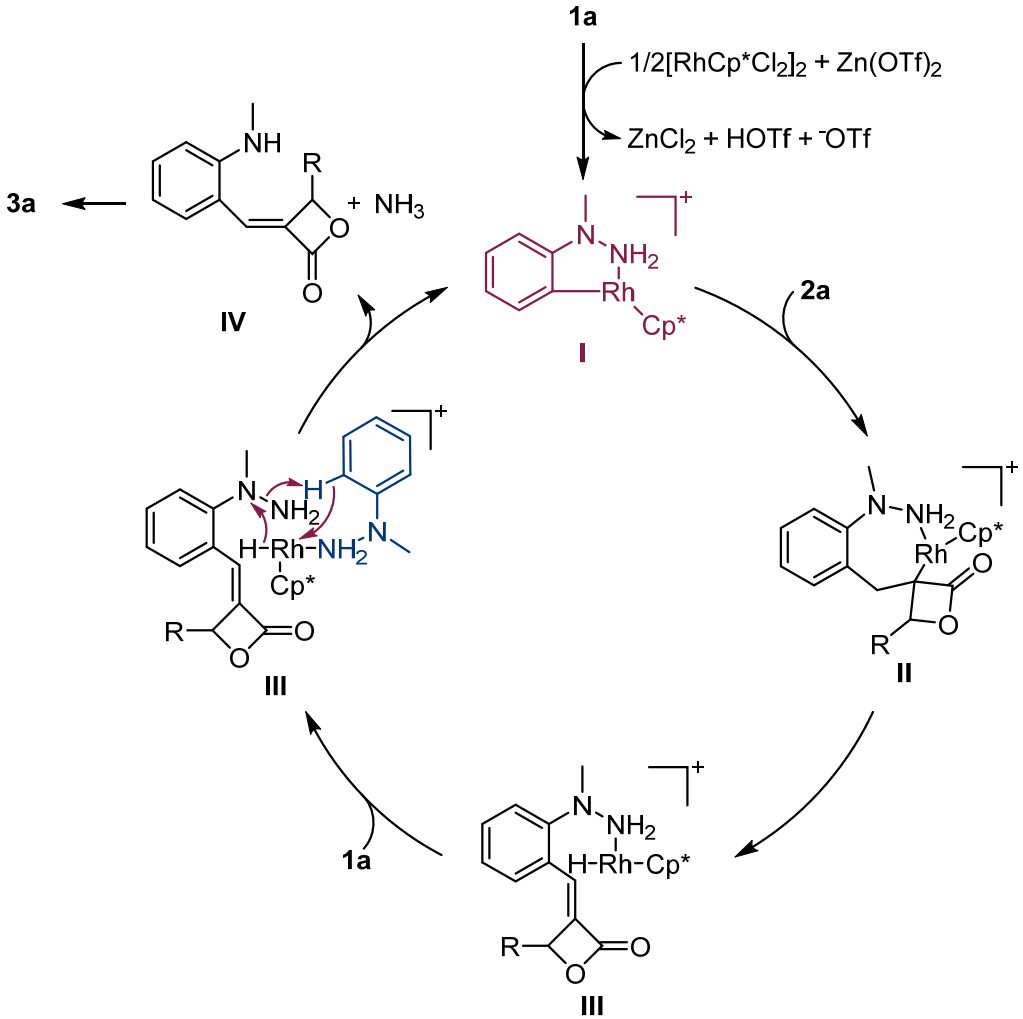

References

(1) Baumer, L.; Sala, G.; Sello, G. Computer-Assisted Organic Synthesis Planning: Effective Bond Polarity as a Guideline to Reactivity. *J. Am. Chem. Soc.* **1991**, *113*, 2494-2500.

(2) Reed, L. H.; Allen, L. C. Bond Polarity Index: Application to Group Electronegativity. *J. Phys. Chem.* **1992**, *96*, 157-164.

(3) Oelkers, B.; Butovskii, M. V.; Kempe, R. F-Element-Metal Bonding and the Use of the Bond Polarity To Build Molecular Intermetalloids. *Chem. Eur. J.* **2012**, *18*, 13566-13579.

(4) Luca, O. R.; Crabtree, R. H. Redox-Active Ligands in Catalysis. *Chem. Soc. Rev.* **2013**, *42*, 1440-1459.

(5) Belkova, N. V.; Epstein, L. M.; Filippov, O. A.; Shubina, E. S. Hydrogen and Dihydrogen Bonds in the Reactions of Metal Hydrides. *Chem. Rev.* **2016**, *116*, 8545-8587.

(6) Singh, S. K.; Eng, J.; Atanasov, M.; Neese, F. Covalency and Chemical Bonding in Transition Metal Complexes: An Ab Initio Based Ligand Field Perspective. *Coord. Chem. Rev.* **2017**, *344*, 2-25.

(7) Elsby, M. R.; Baker, R. T. Strategies and Mechanisms of Metal-Ligand Cooperativity in First-Row Transition Metal Complex Catalysts. *Chem. Soc. Rev.* **2020**, *49*, 8933-8987.

(8) Wheaton, A. M.; Chipman, J. A.; Roy, M. D.; Berry, John. F. Metal-Metal Bond Umpolung in Heterometallic Extended Metal Atom Chains. *Inorg. Chem.* **2022**, *61*, 15058-15069.

(9) Allred, A. L.; Rochow, E. G. A Scale of Electronegativity Based on Electrostatic Force. *J. Inorg. Nucl. Chem.* **1958**, *5*, 264-268.

(10) Seebach, D. Methods of Reactivity Umpolung. *Angew. Chem., Int. Ed.* **1979**, *18*, 239-258.

(11) Murphy, L. R.; Meek, T. L.; Allred, A. L.; Allen, L. C. Evaluation and Test of Pauling's Electronegativity Scale. *J. Phys. Chem. A* **2000**, *104*, 5867-5871.

(12) Mullins, J. J. Six Pillars of Organic Chemistry. *J. Chem. Educ.* **2008**, *85*, 83-87.

(13) Batsanov, S. S. Energy Electronegativity and Chemical Bonding. *Molecules* **2022**, *27*, 8215.

(14) Yu, I. F.; Wilson, J. W.; Hartwig, J. F. Transition-Metal-Catalyzed Silylation and Borylation of C-H Bonds for the Synthesis and Functionalization of Complex Molecules. *Chem. Rev.* **2023**, *123*, 11619-11663.

(15) Adhikari, A.; Chhetri, K.; Rai, R.; Acharya, D.; Kunwar, J.; Bhattarai, R. M.; Jha, R. K.; Kandel, D.; Kim, H. Y.; Kandel, M. R. (Fe-Co-Ni-Zn)-Based Metal-Organic Framework-Derived Electrocatalyst for Zinc-Air Batteries. *Nanomaterials* **2023**, *13*, 2612.

(16) Hassan, M. M. M.; Guria, S.; Dey, S.; Das, J.; Chattopadhyay, B. Transition Metal-Catalyzed Remote C-H Borylation: An Emerging Synthetic Tool. *Sci. Adv.* **2023**, *9*, 3311.

(17) Zhang, G.; Zhang, Q. Cobalt-Catalyzed HAT Reaction for Asymmetric Hydrofunctionalization of Alkenes and Nucleophiles. *Chem. Catal.* **2023**, *3*, 100526.

(18) García-Melchor, M.; Braga, A. A. C.; Lledós, A.; Ujaque, G.; Maseras, F. Computational Perspective on Pd-Catalyzed C-C Cross-Coupling Reaction Mechanisms. *Acc. Chem. Res.* **2013**, *46*, 2626-2634.

(19) Zhou, S.; Wang, J.; Zhang, F.; Song, C.; Zhu, J. A Versatile, Traceless C-H Activation-Based Approach for the Synthesis of Heterocycles. *Org. Lett.* **2016**,

18, 2427-2430.

(20) Zhou, S.; Wang, J.; Wang, L.; Chen, K.; Song, C.; Zhu, J. Co(III)-Catalyzed, Internal and Terminal Alkyne-Compatible Synthesis of Indoles. *Org. Lett.* **2016**, *18*, 3806-3809.

(21) Song, C.; Yang, C.; Zhang, F.; Wang, J.; Zhu, J. Access to the Cinnoline Scaffold via Rhodium-Catalyzed Intermolecular Cyclization under Mild Conditions. *Org. Lett.* **2016**, *18*, 4510-4513.

(22) Wu, W.; Fan, S.; Li, T.; Fang, L.; Chu, B.; Zhu, J. Cobalt-Catalyzed, Directed Intermolecular C-H Bond Functionalization for Multiheteroatom Heterocycle Synthesis: The Case of Benzotriazine. *Org. Lett.* **2021**, *23*, 5652-5657.

(23) Ackermann, L. Carboxylate-Assisted Ruthenium-Catalyzed Alkyne Annulations by C-H/Het-H Bond Functionalizations. *Acc. Chem. Res.* **2014**, *47*, 281-295.

(24) Ujwaldev, S. M.; Harry, N. A.; Divakar, M. A.; Anilkumar, G. Cobalt-Catalyzed C-H Activation: Recent Progress in Heterocyclic Chemistry. *Catal. Sci. Technol.* **2018**, *8*, 5983-6018.

(25) Desai, B.; Patel, M.; Dholakiya, B. Z.; Rana, S.; Naveen, T. Recent Advances in Directed sp^2 C-H Functionalization towards the Synthesis of *N*-Heterocycles and *O*-Heterocycles. *Chem. Commun.* **2021**, *57*, 8699-8725.

(26) Wang, H.; Tang, G.; Li, X. Rhodium(III)-Catalyzed Amidation of Unactivated C(sp^3)-H Bonds. *Angew. Chem., Int. Ed.* **2015**, *54*, 13049-13052.

(27) Jiao, J.; Murakami, K.; Itami, K. Catalytic Methods for Aromatic C-H Amination: An Ideal Strategy for Nitrogen-Based Functional Molecules. *ACS Catal.* **2016**, *6*, 610-633.

(28) Kim, J. H.; Greßies, S.; Glorius, F. Cooperative Lewis Acid/Cp*Co^{III} Catalyzed C-H Bond Activation for the Synthesis of Isoquinolin-3-Ones. *Angew. Chem., Int.*

Ed. **2016**, *55*, 5577-5581.

(29) Xia, J.; Kong, L.; Zhou, X.; Zheng, G.; Li, X. Access to Substituted Propenoic Acids via Rh(III)-Catalyzed C-H Allylation of (Hetero)Arenes with Methyleneoxetanones. *Org. Lett.* **2017**, *19*, 5972-5975.

(30) Bian, M.; Ma, K.; Mawjuda, H.; Yu, X.; Li, X.; Gao, H.; Zhou, Z.; Yi, W. Rhodium(III)-Catalyzed Chemoselective C-H Functionalization of Benzamides with Methyleneoxetanones Controlled by the Solvent. *Org. Biomol. Chem.* **2019**, *17*, 6114-6118.

(31) Zhu, G.; Shi, W.; Gao, H.; Zhou, Z.; Song, H.; Yi, W. Chemodivergent Couplings of *N*-Arylureas and Methyleneoxetanones via Rh(III)-Catalyzed and Solvent-Controlled C-H Activation. *Org. Lett.* **2019**, *21*, 4143-4147.

(32) Xu, Y.; Zhang, L.; Liu, M.; Zhang, X.; Zhang, X.; Fan, X. Synthesis of Benzoazepine Derivatives via Rh(III)-Catalyzed Inert C(sp^2)-H Functionalization and [4+3] Annulation. *Org. Biomol. Chem.* **2019**, *17*, 8706-8710.

(33) Bian, M.; Mawjuda, H.; Gao, H.; Xu, H.; Zhou, Z.; Yi, W. Lossen Rearrangement vs C-N Reductive Elimination Enabled by Rh(III)-Catalyzed C-H Activation/Selective Lactone Ring-Opening: Chemodivergent Synthesis of Quinolinones and Dihydroisoquinolinones. *Org. Lett.* **2020**, *22*, 9677-9682.

(34) Zhou, Z.; Bian, M.; Zhao, L.; Gao, H.; Huang, J.; Liu, X.; Yu, X.; Li, X.; Yi, W. 2H-Chromene-3-Carboxylic Acid Synthesis via Solvent-Controlled and Rhodium(III)-Catalyzed Redox-Neutral C-H Activation/[3+3] Annulation Cascade. *Org. Lett.* **2018**, *20*, 3892-3896.

(35) Yu, X.; Chen, K.; Wang, Q.; Guo, S.; Zha, S.; Zhu, J. Associative Covalent Relay: An Oxadiazolone Strategy for Rhodium(III)-Catalyzed Synthesis of

Primary Pyridinylamines. *Angew. Chem., Int. Ed.* **2017**, *56*, 5222-5226.

(36) Qi, B.; Li, L.; Wang, Q.; Zhang, W.; Fang, L.; Zhu, J. Rh(III)-Catalyzed Coupling of *N*-Chloroimines with *α*-Diazo-*α*-Phosphonoacetates for the Synthesis of 2*H*-Isoindoles. *Org. Lett.* **2019**, *21*, 6860-6863.

Acknowledgments

J.Z. gratefully acknowledges support from the National Natural Science Foundation of China (52073141 and 22275083) and the Department of Science and Technology of Jiangsu Province (BE2022839).